JOURNAL OF Applied Polymer SCIENCE

Flexible and Flame-Retardant S-SEB-S Triblock Copolymer/PPE Nano-Alloy

Yoshifumi Araki,[1] Yukari Hori,[1] Katsumi Suzuki,[1] Hiroshi Shirai,[1] Kiyoo Kato,[1] Hiromu Saito[2]

[1]Asahi Kasei Chemicals Corporation, Kawasaki-ku, Kawasaki-city, Kanagawa 210-0863, Japan

[2]Department of Organic and Polymer Materials Chemistry, Tokyo University of Agriculture and Technology, Koganei-shi, Tokyo 184-8588, Japan

Correspondence to: Y. Araki (E-mail: araki.yb@om.asahi-kasei.co.jp)

ABSTRACT: We observed that modified polyphenylene ether (PPE) was solubilized in thermoplastic styrenic elastomer (TPS) and that a two-phase lacy structure formed on nanometer scales when the TPS composition was 67 wt % and modified PPE and polystyrene-*block*-poly(styrene-*co*-ethylene-*co*-butylene)-*block*-polystyrene (S-SEB-S triblock copolymer) were blended. However, the molecular weight of the outer PS block segments M_{outPS} and the content of the outer PS block segments ϕ_{outPS} were <10,000 g/mol and 20 wt %, respectively. The resulting S-SEB-S/modified PPE nano-alloy exhibited both flexibility and flame retardancy, unlike other materials, where a trade-off exists between these two properties; that is, the flame retardancy was excellent when the phosphorus additive was present. This combination of properties might be attributed to the two-phase nanometer-scale structure consisting of flame-retardant styrene/PPE domains and a continuous soft, lacy SEB matrix. The results for polystyrene-*block*-poly(ethylene-*co*-butylene)-*block*-polystyrene (S-EB-S triblock copolymer)/modified PPE blends were presented for comparison. © 2014 Wiley Periodicals, Inc. J. Appl. Polym. Sci. **2014**, *131*, 40446.

KEYWORDS: structure-property relations; blends; mechanical properties; flame retardance; nanostructured polymers

Received 28 September 2013; accepted 15 January 2014

DOI: 10.1002/app.40446

INTRODUCTION

Flexible flame-retardant materials are desirable for use in wire coatings for flexible wire insulation, USB cables, cell-phone chargers/adapters, and internal wiring. Poly(2,6-dimethyl-l,4-phenylene ether) (PPE) is an excellent flame-retardant material due to its high limiting oxygen index, halogen-free, compliant with environmental regulations, high heat distortion temperature, and low specific gravity[1–4]; however, it is brittle and unprocessable. Due to its unprocessability, modified PPE, a blend of PPE and PS, is usually used for industrial products, but the flame retardancy of modified PPE is insufficient without including flame retardant additive.[5] The mechanical properties and processability of PPE have been improved frequently by blending it with thermoplastic styrenic elastomers (TPSs) consisting of outer glassy polystyrene (PS) block segments and middle rubbery blocks such as polystyrene-*block*-polybutadiene-*block*-polystyrene (S-B-S triblock copolymer) and its hydrogenated version, polystyrene-*block*-poly(ethylene-*co*-butylene)-*block*-polystyrene (S-EB-S triblock copolymer),[6–12] because PPE is solubilized by PS block segments in TPS.[13,14] However, these blends are usually limited to PPE-rich compositions to maintain the toughness, the inherent heat resistance and flame retardancy, whereas these blends are inflexible and inferior processability. Blend flexibility improves as the PPE component decreases; however, the PPE phase separates from TPS on the micrometer scale when the molecular weight and/or the content of styrene segments of TPS is low.[15,16] In addition, flame-retardant properties are inferior for TPS-rich blends with commercially available modified PPE included flame retardant. In contrast, the modified PPE can be solubilized with TPS and exhibit flame-retardant properties at low PPE compositions when the molecular weight and/or the content of the outer PS segments are high and flame retardant additive is included; however, these blends are not flexible. Hence, the fabrication of materials that are both flexible and flame retardant has been difficult due to the trade-off between these properties.

A polystyrene-*block*-poly(styrene-*co*-butadiene)-*block*-polystyrene (S-SB-S ABA-type triblock copolymer) was recently developed through living alkyllithium-initiated polymerization. The tensile strength and moduli of this S-SB-S copolymer distinctly increased with the degree of hydrogenation because of greater segregation of the microphase structure.[17] Despite containing >50 wt % styrene, hydrogenated S-SB-S triblock copolymer (S-SEB-S) exhibited softness and flexibility as well as excellent

Table I. Molecular Structures of TPSs

			S-EB-S (S30)	S-EB-S (S67)	S-SEB-S (S20)
Structure of TPSs	Total St content of two outer PS blocks	(wt%)	30	67	20
	Total St content of middle block	(wt%)	0	0	47
	Total St content	(wt%)	30	67	67
	Schematic molecular structure of HTPS	*1			
Molecular weight	*Mn Mw*	(g/mol)	70,000 74,000	53,000 56,000	99,000 105,000
Molecular weight of outer PS block	*Mn*	(g/mol)	10,500	17,800	9,900

*1 PS block styrene-*co*-butadiene random copolymer block (mol ratio: styrene / butadiene = 42.5/57.5)

shock absorption, abrasion resistance, and filler compatibility.[18] The softness and flexibility of these copolymers are attributed to their microphase structure, where hard PS block segments form microdomains in a continuous matrix of soft hydrogenated SB block segments.[17] Because the middle block of S-SEB-S contains styrene, this copolymer is expected to solubilize PPE and to exhibit flexibility and flame retardancy in blends.

In this study, we used transmission electron microscopy (TEM) and small-angle X-ray scattering (SAXS) measurements to investigate the morphology of S-SEB-S/modified PPE blends and the solubilization of modified PPE in S-SEB-S. The trade-off between flexibility and flame retardancy is discussed in this article in terms of the structure. In addition, results for S-EB-S blends with different molecular weight of the outer PS block segments M_{outPS} and content of the outer PS block segments ϕ_{outPS} values are presented for comparison.

EXPERIMENTAL

The S-EB-S and S-SEB-S triblock copolymers were prepared in two-stage processes where S-B-S and S-SB-S were synthesized, and their double bonds were subsequently hydrogenated to form S-EB-S and S-SEB-S, respectively. The syntheses of S-B-S and S-SB-S were performed sequentially by anionic polymerization using *n*-butyl lithium as an initiator in cyclohexane solvent at 80°C, as described by Yoshida and Friedrich.[19] The first PS block was polymerized from styrene monomer. Next, either butadiene monomer or both styrene and butadiene monomers were added at a constant rate to form the middle blocks of S-B-S or S-SB-S, respectively. Finally, styrene monomer was added to polymerize the second PS outer block. Because butadiene monomer reacts preferentially with lithium groups rather than with styrene,[20] we carefully conducted the polymerization process to maintain a constant styrene-to-butadiene ratio in the SB middle block. Here, the mole ratio of styrene to butadiene in the middle block was between 42.5 and 57.5. We added *N,N,N′,N′*-tetramethylethylenediamine to the solution at the beginning of the reaction process. The hydrogenation of S-B-S and S-SB-S was performed using a titanocene catalyst in cyclohexane solvent. Double bonds in the B and SB block segments were hydrogenated to obtain S-EB-S and S-SEB-S, respectively. The molecular structure and molecular weight of the S-EB-S and S-SEB-S triblock copolymers are shown in Table I. Here, the molecular weight of the outer PS block was measured by GPC after (1) taking from the solution after polymerization, and then (2) degradating butadiene in the middle block by using osmic acid in *tert*-butanol before the hydrogenation.[21] The conversion estimated by Gas chromatography is above 99%.[17,19]

In this study, the modified PPE was a commercial product, X1010 (Asahi Kasei Chemicals, Tokyo, Japan), which is a blend of 70 wt % PPE (M_n = 18,000 g/mol) and PS (M_n = 200,000 g/mol). The S-EB-S or S-SEB-S triblock copolymers were melt-mixed with modified PPE using a twin-screw extruder with a 32-mm screw diameter (TEX30α, The Japan Steel Works, Tokyo, Japan), a rotation speed of 250 rpm, and an operating temperature of 250°C. Film specimens with a thickness of 2 mm were press molded at 220°C.

The stress–strain curves of the film specimens were obtained at room temperature using an Instron-type tensile-testing machine (VES05D, Toyo Seiki Seisaku-sho, Tokyo, Japan). The initial length and elongation rate were 40 mm and 500 mm/min, respectively.

Flame retardancy was evaluated on the basis of the flame-out time using the UL VW-1 vertical-wire flame test (UL 1581). To carry out this flame test, a phosphorus-based flame retardant was used to form 60/30/10 TPS/PPE/flame retardant blends by weight. The flame retardant was tetraphenyl resorcinol bis(diphenylphosphate) manufactured by Daiichi Chemical Industry; an extruder was used to coat conductive wire specimens.

For the TEM observations, ultrathin sections ~70 nm thick were cut from the film specimens with a cryomicrotome. Each section was stained with ruthenium tetraxide (RuO_4) vapor for 5 min at room temperature. The morphology was observed using a transmission electron microscope (JEM 1230, Jeol, Tokyo, Japan) with an acceleration voltage of 80 kV.

RESULTS AND DISCUSSION

Figure 1 shows the TEM micrographs of TPSs of S-EB-S and S-SEB-S. These TPSs consist of middle rubbery blocks and

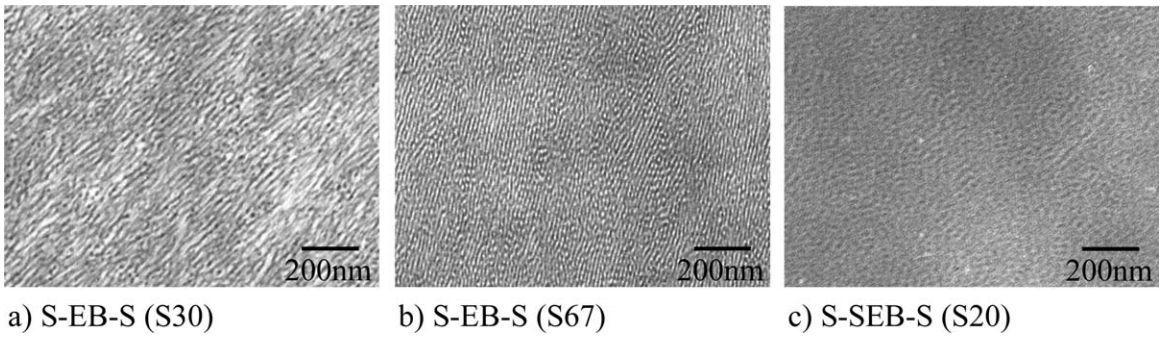

Figure 1. TEM micrographs of TPSs of S-EB-S and S-SEB-S.

outer glassy PS block segments with different PS contents, that is, S-EB-S (S30; the content of the outer PS block segments $\phi_{outPS} = 30$ wt %), S-EB-S (S67; $\phi_{outPS} = 67$ wt %), and S-SEB-S (S20; $\phi_{outPS} = 20$ wt %). Two-phase cylindrical microdomains with diameters of several tens of nanometers are dispersed throughout the matrix in the S-EB-S (S30) and the S-EB-S (S67) [Figures 1(a,b)], whereas two-phase spherical domains with diameters of several tens of nanometers are dispersed throughout the matrix in the S-SEB-S (S20) [Figure 1(c)]. Because RuO_4 preferentially stains styrene block segments, the dark matrix regions in S-EB-S (S67) can be identified as hard outer PS block segments [Figure 1(b)], whereas the light matrix regions in S-EB-S (S30) and S-SEB-S (S20) are soft EB and SEB middle segments, respectively [Figures 1(a,c)]. Thus, cylindrical and spherical hard PS microdomains are dispersed throughout the continuous rubbery matrix in S-EB-S (S30) and S-SEB-S (S20), respectively, whereas cylindrical rubbery microdomains are dispersed throughout the continuous hard PS matrix in S-EB-S (S67).

The TPSs illustrated in Figure 1 were blended with modified PPE. Figure 2 shows TEM micrographs of 67/33 TPS/modified PPE blends. A three-phase structure is observed in the S-EB-S (S30)/modified PPE blend [Figure 2(a)]. Domains with several hundred nanometers in size are dispersed in a large matrix that is several micrometers in diameter. The cylinder-like structure of this matrix is similar to the structure observed in S-EB-S (S30). Because RuO_4 preferentially stains modified PPE rather than S-EB-S (S30) included EB block segments, the dark domains can be identified as modified PPE, whereas the light matrix region with cylinder-like structure can be assigned to S-EB-S microdomains. Thus, the three-phase structure of the S-EB-S (S30)/modified PPE blend is attributed to the macrophase separation of S-EB-S (S30) and modified PPE. Hence, S-EB-S (S30)/modified PPE blend is considered to be an S-EB-S/PPE macro-alloy. Because modified PPE can be solubilized with PS block segments in TPS when ϕ_{outPS} is high, macrophase separation occurs when ϕ_{outPS} is too low ($\phi_{outPS} = 30$ wt %) to solubilize modified PPE at a TPS composition of 67 wt %.

Two-phase cylinder-like structures are observed in the S-EB-S (S67)/modified PPE blend [Figure 2(b)], whereas a two-phase lacy structure is present in the S-SEB-S (S20)/modified PPE blend [Figure 2(c)]. The nanometer scale of this structure indicates that a nano-alloy with two-phase structure was formed by blending modified PPE with the TPSs of S-EB-S (S67) and S-SEB-S (S20). Hence, the blends of modified PPE with S-EB-S (S67) and S-SEB-S (S20) were considered to be S-EB-S (S67)/PPE and S-SEB-S (S20)/PPE nano-alloys, respectively. The two-phase structures of these blends are larger than the structures in the TPSs. The scale of these two-phase structures can be attributed to the solubilization of modified PPE in PS block segments, that is, the modified PPE is inserted preferentially into the PS phase of TPSs. Because RuO_4 preferentially stains styrene and PPE, the dark matrix regions in the S-EB-S (S67)/PPE nano-alloy can be identified as the mixed phase of PS and PPE, whereas the light matrix regions in the S-SEB-S (S20)/PPE nano-alloy are the soft SEB phase. Thus, soft EB domains are dispersed throughout the continuous hard PS/PPE matrix in the S-EB-S (S67)/PPE nano-alloy, and hard PS/PPE domains are dispersed throughout the continuous soft, lacy SEB matrix in the S-SEB-S (S20)/PPE nano-alloy. The structure of the S-SEB-S

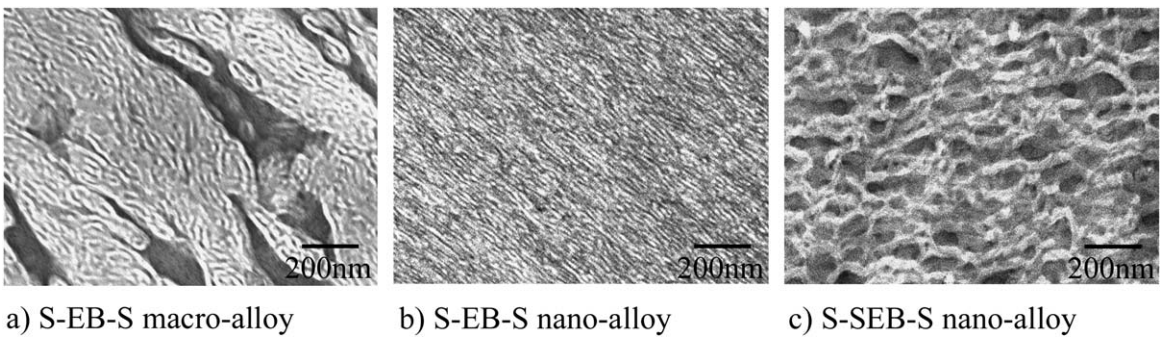

Figure 2. TEM micrographs of 67/33 TPS/modified PPE blends.

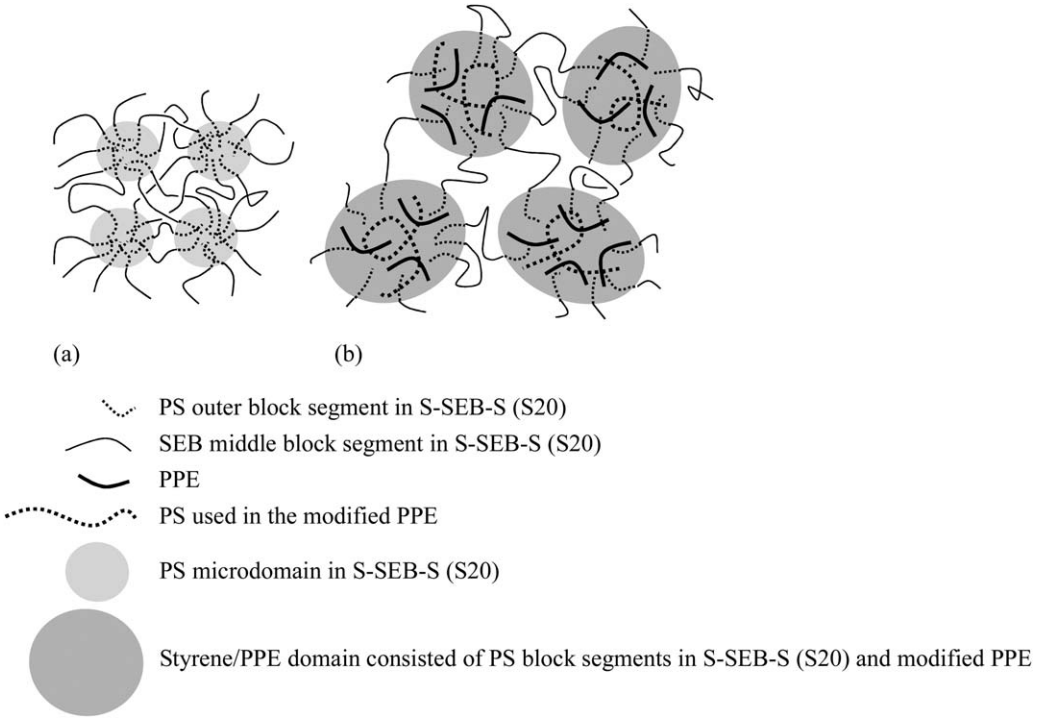

Figure 3. Schematic illustration of microphase structure: (a) S-SEB-S (S20) and (b) S-SEB-S (S20)/PPE nano-alloy.

(S20)/PPE nano-alloy differed from that of S-SEB-S (S20), whereas the cylinder-like structure of the S-EB-S (S67)/PPE nano-alloy was very similar to that of S-EB-S (S67). The lacy structure in the S-SEB-S (S20)/PPE nano-alloy consists of domains surrounded by a lacy matrix; that is, the size of the domain and the diameter of the lacy matrix are ~100 and 30 nm, respectively. The microphase structure of the S-SEB-S (S20)/PPE nano-alloy was coarser than the structure of the S-EB-S (S67)/PPE nano-alloy; however, the microphase structure of S-SEB-S (S20)/PPE nano-alloy did not grow to the micrometer scale despite long annealing, which suggests that phase separation does not proceed at the micrometer scale. Such two-phase lacy structure is similar to that observed by Puskas et al. observed in polystyrene-*block*-polyisobutylene-*block*-polystyrene (S-IB-S triblock copolymer)/PPE blends. The lacy structure is observed in S-IB-S/PPE blends at high PPE composition,[12] while that is observed in S-SEB-S (S20)/modified PPE blends at high TPS composition.

Thus, the S-SEB-S (S20)/PPE nano-alloy formed when modified PPE was inserted into the PS domains of TPS, although the molecular weight of the outer PS segments M_{outPS} and the content of the outer PS block segments ϕ_{outPS} were both low ($M_{outPS} = 9900$ g/mol and $\phi_{outPS} = 20$ wt %). PPE is well known to be immiscible with TPSs at high TPS compositions when PS outer blocks have a low M_{outPS} of <10,000 g/mol and a low ϕ_{outPS} of <52 wt %; for example, macrophase separated structure is observed in polystyrene-*block*-poly(ethylene-*co*-butylene)-*block*-polystyrene/PPE blends at $M_{outPS} = 6000$ g/mol and $\phi_{outPS} = 16$ vol %,[15] and in polystyrene-*block*-polyisoprene /PPE blends at $M_{outPS} = 27{,}000$ g/mol and $\phi_{outPS} = 52$ wt %.[16] To the best of our knowledge, our observation of 67/33 S-SEB-S/modified PPE is the first reported case of a PPE nano-alloy solubilized with TPS where the major component of TPS has a low M_{outPS} and a low $\phi_{outPS.}$ Because S-SEB-S contains styrene in its middle block, the Flory–Huggins χ-parameter between PPE and S-SEB-S is low. Hence, PPE is solubilized with S-SEB-S and can be inserted into outer PS blocks, and a nano-alloy can be obtained without phase separation on a micrometer scale as schematically shown in Figure 3, although PPE is immiscible with the SEB random copolymer that is a constituent of the middle block segments of S-SEB-S and M_{outPS} and ϕ_{outPS} are less than 10,000 g/mol and 52 wt %, respectively. To understand this structure more quantitatively, SAXS results were analyzed.

Figure 4 shows SAXS profiles of TPSs and the TPS/modified PPE blends presented in Figures 1 and 2. A peak is observed in the spectra of S-EB-S (S30) and S-EB-S (S67), which indicates the presence of two-phase structures with periodic microdomains [Figure 3(a)]. The periodic distance between the microdomains, d, can be calculated using Bragg's law ($d = 2\pi/q_{max}$), where q_{max} is the scattering vector of the peak maximum. The calculated periodic distances in S-EB-S (S30) and S-EB-S (S67) were ~29 and 25 nm, respectively. The S-EB-S peak was shifted to lower angles when modified PPE was blended with S-EB-S. For S-EB-S (S67), d increased when S-EB-S was blended with modified PPE, that is, d was 25 and 28 nm for S-EB-S (S67) and S-EB-S (S67)/PPE nano-alloys, respectively. This result indicates that the periodicity of the microdomains was increased by blending modified PPE and suggests that modified PPE was inserted into the PS matrix of S-EB-S (S67). Because the ϕ_{outPS} is large and because there is more PS than PPE, blending PPE causes a small change in the microstructure of S-EB-S (S67), even though PPE is inserted into the PS matrix of S-EB-S

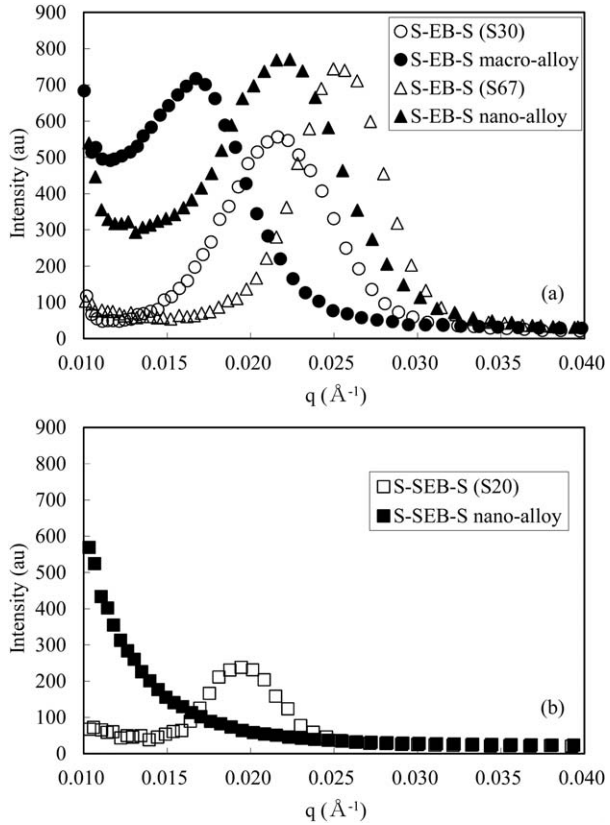

Figure 4. SAXS profiles: (a) S-EB-Ss and S-EB-S/modified PPE blends and (b) S-SEB-S and S-SEB-S/modified PPE blend.

(S67). The *d* was also larger in the S-EB-S (S30)/PPE macro-alloy than in S-EB-S (S30), that is, the *d* values of S-EB-S (S30) and the S-EB-S (S30)/PPE macro-alloy were 29 and 38 nm, respectively. This result suggests that the modified PPE is inserted partially into the PS domain of S-EB-S (S30), although the phase separation of PPE and S-EB-S (S30) occurs on the micrometer scale, as demonstrated in Figure 2(a).

No peak was observed in the SAXS profile shown in Figure 4(b), and the SAXS intensity decreased monotonously with decreasing angle in the S-SEB-S/PPE nano-alloy; however, a peak was observed in the profile of S-SEB-S (S20). These results indicate that the blending of PPE caused the periodic distance between the microdomains of S-SEB-S (S20) to increase from 32 nm to above the limit of SAXS measurement of 80 nm. This observation suggests that the microphase separation structure of S-SEB-S (S20) changed to a larger structure when modified PPE was inserted into the PS domain in S-SEB-S (S20), as demonstrated in Figures 1(c) and 2(c). The structure of the S-SEB-S (S20)/PPE nano-alloy was larger than the structure of the S-EB-S (S67)/PPE nano-alloy. The larger structure of the S-SEB-S (S20)/PPE nano-alloy might be attributed to the coalescence of S-SEB-S (S20) phases because of the low ϕ_{outPS} ($\phi_{outPS} = 20$ wt %), although coalescence did not lead to the formation of a three-phase structure at the micrometer scale.

Figure 5 shows the stress–strain properties of TPSs and the TPS/modified PPE blends whose structures are presented in Figures 1–4; that is, two-phase domain structures with diameters of several tens of nanometers, a three-phase structure consisting of domains several hundred nanometers in size dispersed in a large matrix of cylinder-like structure, a two-phase cylinder-like structure with a diameter of several tens of nanometers, and a two-phase lacy structure with domains of about 100 nm, are observed in TPSs, S-EB-E (S30)/PPE macro-alloy, S-EB-S (S67)/PPE nano-alloy, and S-SEB-S (S20)/PPE nano-alloy, respectively. For modified PPE and S-EB-S (S67), the stress increased steeply to >40 MPa and broke at a strain <0.07, indicating brittleness. The S-EB-S (S67)/PPE nano-alloy obtained by blending S-EB-S (S67) with modified PPE was also brittle, and it broke at a strain <0.03. Conversely, the initial stress of S-EB-S (S30) and S-SEB-S (S20) increased gradually with strain in the low-strain region and then sharply increased at strains >1.5 up to the breaking point. Similar features (low strength at low strains, sharp increases in stress for high strains, and high elongation at break) were observed for crosslinked rubbers. The initial modulus and strength of S-EB-S (S30) and S-SEB-S (S20) increased and the strain at break decreased when the TPSs were blended with modified PPE. Nevertheless, the S-SEB-S (S20)/PPE nano-alloy obtained by blending S-SEB-S (S20) with modified PPE exhibited flexible behavior similar to that of crosslinked rubbers. The strength of the S-SEB-S (S20)/PPE nano-alloy was less than that of the S-EB-S (S30)/PPE macro-alloy for strains <0.3, indicating that the initial modulus of the S-SEB-S (S20)/PPE nano-alloy was less than that of the S-EB-S (S30)/PPE macro-alloy. This flexible behavior of the S-SEB-S/PPE nano-alloy might be attributable to the existence of the soft SEB matrix, as shown in Figure 2(c).

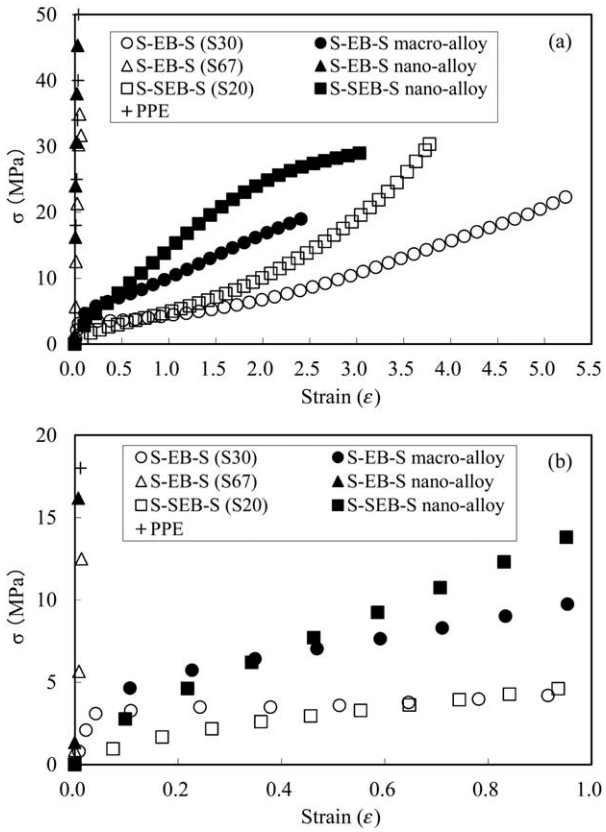

Figure 5. Stress-strain curves of TPSs, PPE, and the TPS/modified PPE blends: (a) high-strain region and (b) low-strain region.

Table II. Work of Fracture of Modified PPE, TPSs, and TPS/Modified PPE Blends

	Work of fracture (MJ/m^3)	
	neat polymer	TPS/modified PPE blends
modified PPE	2.9	-
S-EB-S (S30)	53.7	27.5
S-EB-S (S67)	1.5	0.9
S-SEB-S (S20)	43.2	55.9

Table III. Flame-Out Times of TPS/Modified PPE/Flame Retardant Blends Obtained via the VW-1 Vertical-Wire Flame Test

	S-EB-S (S30)	S-EB-S (S67)	S-SEB-S (S20)
Flame-out time at first time (sec)	>60	16	18

By integrating the curve of Figure 5, the work of fracture was obtained. The work of fracture of modified PPE and TPSs, and the TPS/modified PPE blends are shown in Table II. The interesting result here is that the work of fracture of the S-SEB-S (S20)/PPE nano-alloy is much larger than those of S-EB-S (S30)/PPE macro-alloy though the work of fracture of the S-SEB-S (S20) is smaller than that of S-EB-S (S30). This indicates that the strain energy of the S-SEB-S (S20)/PPE nano-alloy was large; that is, blending with PPE caused a small decrease in the elongation at break, and the S-SEB-S (S20)/PPE nano-alloy was much stronger during elongation than S-SEB-S (S20) and the S-EB-S (S30)/PPE macro-alloy. This decrease in elongation associated with blending brittle PPE can be suppressed by the dispersion of stress concentrations induced by the presence of a two-phase structure at the nanometer scale with a large interphase area. The strength of the S-SEB-S (S20)/PPE nano-alloy might be attributed to the transmittance of stress in hard domains because the soft matrix exhibited a thin lacy structure, as shown in Figure 2(c).

The flame retardancy of materials is evaluated by the oxygen index value, and materials with high flame retardancy are classified by oxygen index values >21.[22] The oxygen index values of poybutadiene, PS, and modified PPE are 18, 18, and 30, respectively.[22] As expected from the oxygen index value, the flame retardant properties are inferior for S-EB-S and S-SEB-S and high for modified PPE. Table III shows the flame-out times of the S-EB-S (S30)/PPE macro-alloy, the S-EB-S (S67)/PPE nano-alloy and the S-SEB-S (S20)/PPE nano-alloy obtained via the VW-1 vertical-wire flame test. To conduct this flame test, we added a phosphorus-based flame retardant to the blends because the flame retardancy of the modified PPE is insufficient.[5] The flame-out time of the S-EB-S (S30)/PPE macro-alloy was longer than 60 s, suggesting that the S-EB-S (S30)/PPE macro-alloy continues to combust without extinguishing the flame. However, the flame-out times of the S-EB-S (S67)/PPE nano-alloy and the S-SEB-S (S20)/PPE nano-alloy were <20 s, suggesting that the flame was extinguished before burning out. These results indicate that the S-EB-S (S67)/PPE nano-alloy and S-SEB-S (S20)/PPE nano-alloy exhibit high flame retardancy, whereas the flame-retardant property of the S-EB-S (S30)/PPE macro-alloy is inferior.

Figure 6 shows optical micrographs of the surface of the S-EB-S (S30)/PPE macro-alloy and S-SEB-S (S20)/PPE nano-alloy obtained after the flame was extinguished with water during the VW-1 vertical-wire flame test (Table III). The surface of the S-EB-S (S30)/PPE macro-alloy was burned nonuniformly and was deformed by the combustion. In contrast, the surface of the S-SEB-S (S20)/PPE nano-alloy was almost flat, with little deformation by combustion.

These results show that the S-SEB-S (S20)/PPE nano-alloy exhibited high flame retardancy and that the flame could be extinguished before burning out, whereas the S-EB-S (S30)/PPE macro-alloy combusted without extinguishing the flame, as demonstrated in Table III. The TPS with a low oxygen index can be easily combusted. In contrast, PPE exhibits high flame retardancy because of its self-extinguishing property. Hence, the combustion of the TPS would be suppressed if it was blended with PPE. However, when a large rubbery matrix with a low

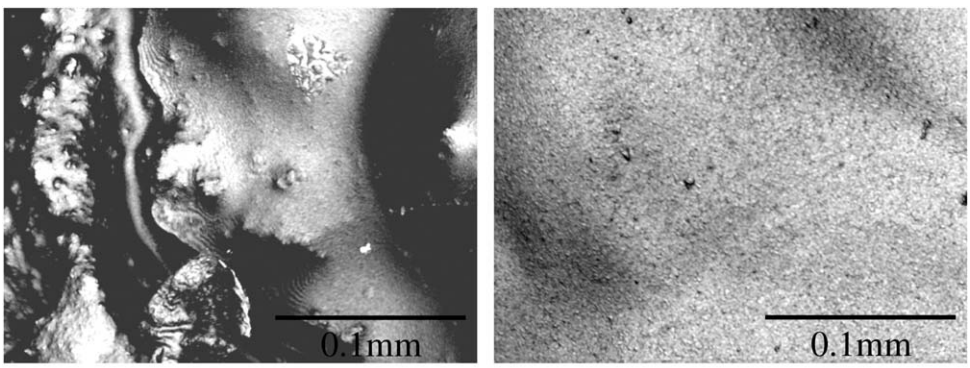

Figure 6. Optical micrographs of surface of the TPS/modified PPE/flame retardant blends obtained after extinguishing the flame by water during the VW-1 vertical-wire flame test.

oxygen index exists at the micrometer scale, as in the case of the S-EB-S (S30)/PPE macro-alloy, the matrix can be combusted easily by nonuniform burning. Then, uniform char cannot form, flammable decomposition gas is emitted, combustion continues, and, finally, it burns out without extinguishing the flame. In contrast, when a rubbery matrix with a low oxygen index is thinner and smaller than the flame-retardant hard domain, as in the case of the S-SEB-S (S20)/PPE nano-alloy, both the matrix and the domain are combusted uniformly. Then, uniform char can form, flammable decomposition gas is not emitted, combustion does not continue, and the flame is extinguished before it burns out. These results, combined with the results in Figure 6, indicate that the S-SEB-S (S20)/PPE nano-alloy exhibits both flexibility and flame-retardant properties, although it has been difficult until now for a single material to exhibit both properties because of the trade-off between flexibility and flame retardancy; for example, the S-EB-S (S30)/PPE macro-alloy was flexible, but its flame-retardant property was inferior, whereas the S-EB-S (S67)/PPE nano-alloy exhibited flame retardancy but was brittle.

CONCLUSIONS

We obtained a material that was both flexible and flame-retardant by blending S-SEB-S (the content of the outer PS block segments $\phi_{outPS} = 20$ wt %) with modified PPE at a S-SEB-S composition of 67 wt %, whereas this combination of properties could not be obtained for blends of S-EB-S and modified PPE. A two-phase lacy structure at the nanometer scale formed in the blend, suggesting that PPE could be solubilized with S-SEB-S and that the modified PPE might be inserted into the PS domains of the S-SEB-S, although the molecular weight and the content of the outer PS block segments were <10,000 and 20 wt %, respectively; such blends usually phase-separate at the micrometer scale. Overcoming the trade-off between flexibility and flame retardancy is attributed to the two-phase structure at the nanometer scale, which consists of flame-retardant styrene/PPE domains in a continuous soft, lacy SEB matrix. Our recent results for simultaneous measurements of stress and birefringence[23,24] revealed that the S-SEB-S/modified PPE nano-alloy orients in a two-step process, that is, both the rubbery SEB matrix and the glassy domains are oriented at low strains, and then only the rubbery SEB matrix is oriented at high strains.[25] Such characteristic deformation behavior might be the origin of the flexibility of the S-SEB-S/modified PPE nano-alloy.

REFERENCES

1. Hay, A. S. *J. Polym. Sci. Part A: Polym. Chem.* **1998**, *36*, 505.
2. Wang, X.; Feng, W.; Li, H.; Ruckenstein, E. *Polymer* **2002**, *43*, 1, 37.
3. Boscoletto, A. B.; Checchin, M.; Milan, L.; Pannocchia, P.; Tavan, M.; Camino, G.; Luda, M. P. *J. Appl. Polym. Sci.* **1998**, *67*, 13, 2231.
4. Boscoletto, A. B.; Checchin, M.; Tavan, M.; Camino, G.; Costa, L.; Luda, M. P. *J. Appl. Polym. Sci.* **1994**, *53*, 1, 121.
5. Feldmann, H.; Steinert, P. *Kunststoffe-German Plastic* **1990**, *80*, 10, 36.
6. Tucker, P. S.; Barlow, J. W.; Paul, D. R. *Macromolecules* **1988**, *21*, 6, 1678.
7. Mazard, C.; Benyahia, L.; Tassin, J. F. *Polym. Int.* **2003**, *52*, 4, 514.
8. Tucker, P. S.; Barlow, J. W.; Paul, D. R. *Macromolecules* **1988**, *21*, 9, 2794.
9. Deanin, R. D.; Lunn, P. *Annu. Tech. Conf.* **2000**, *58*, 2, 2113.
10. Chiu, H. T.; Hwung, D. S. *Eur. Polym. J.* **1994**, *30*, 10, 1191.
11. Schellenberg, J. *J. Appl. Polym. Sci.* **1977**, *64*, 9, 1835.
12. Puskas, J. E.; Kwon, Y.; Altstadt, V.; Kontopoulou, M. *Polymer* **2007**, *48*, 2, 590.
13. Shultz, A. R.; Gendron, B. M. *J. Appl. Polym. Sci.* **1972**, *16*, 2, 461.
14. Machate, C.; Lohmar, J.; Droscher, M. *Makromol. Chem.* **1990**, *191*, 12, 3011.
15. Izumoto, T.; Umeda, H.; Sakurai, S.; Masamoto, J.; Nomura, S.; Kitagawa, Y.; Suda, Y. *Sen'i Gakkaishi* **1999**, *55*, 1, 54.
16. Hashimoto, T.; Kimishima, K.; Hasegawa, H. *Macromolecules* **1991**, *24*, 5704.
17. Araki, Y.; Shimizu, D.; Hori, Y.; Nakatani, K.; Saito, H. *Polym. J.* **2013**, *45*, 1140.
18. Sasagawa, M.; Shiraki, T.; Takayama, S.; Sasaki, S.; Suzuki, K.; Hisasue, T.; Moritou, K. U.S. Pat. 7,964,674 (**2011**).
19. Yoshida, J.; Friedrich, C. *Macromolecules* **2005**, *38*, 7164.
20. Halasa, A. F.; Massie, J. M.; Ceresa, R. J. In The Science and Technology of Rubber, 3rd ed.; Mark, J. E., Erman, B., Eirich, F. R., Eds.; Elsevier Academic Press: Amsterdam, **2005**; Chapter 11, p 497–528.
21. Kalthoff, I. M.; Lee, T. S.; Carr, C. W. *J. Polym. Sci.* **1946**, *1*, 5, 429.
22. Gordon, L. N. In Fire and Polymers II; Gordon, L. N., Ed.; American Chemical Society: Washington, DC, **1995**; Chapter 1, p 1–26.
23. Shimizu, K.; Saito, H. *J. Polym. Sci. Part B: Polym. Phys.* **2009**, *47*, 715.
24. Shimizu, K.; Saito, H. *Polym. J.* **2009**, *41*, 562.
25. Araki, Y.; Nakatani, K.; Hori, Y.; Suzuki, K.; Shirai, H.; Kato, K.; Saito, H. *Polym. J.*, to appear.